In Quest of Virtual Tests for Structural Composites

Brian Cox, *et al.*

Science **314**, 1102 (2006);
DOI: 10.1126/science.1131624

REVIEW

In Quest of Virtual Tests for Structural Composites

Brian Cox[1]* and Qingda Yang[2]

The difficult challenge of simulating diffuse and complex fracture patterns in tough structural composites is at last beginning to yield to conceptual and computational advances in fracture modeling. Contributing successes include the refinement of cohesive models of fracture and the formulation of hybrid stress-strain and traction-displacement models that combine continuum (spatially averaged) and discrete damage representations in a single calculation. Emerging hierarchical formulations add the potential of tracing the damage mechanisms down through all scales to the atomic. As the models near the fidelity required for their use as virtual experiments, opportunities arise for reducing the number of costly tests needed to certify safety and extending the design space to include material configurations that are too complex to certify by purely empirical methods.

Predicting the failure of materials is one of the oldest problems of engineering (*1*) and one of the least perfectly solved. Even in modern times, after a century of the formal study of fracture mechanics (*2*, *3*) and the advent of computational stress analysis, predictions remain closely tied to empirical data gathering. In the case of structures upon whose integrity human lives depend, the burden of testing to prove safety is immense: A typical large airframe, for example, currently requires ~10^4 tests of material specimens, along with tests of components and structures up to entire tails, wing boxes, and fuselages, to achieve safety certification (*4*). Although stress analysis is an excellent tool for predicting the distribution of loads throughout the structure when its behavior is linear-elastic, once damage begins, prediction becomes problematic. The fundamental difficulty is that damage in tough engineering materials (excluding brittle materials such as glass) involves extremely complicated nonlinear processes acting from the atomic scale (e.g., dislocations and bond rupture) through the microscale (e.g., microcracking, crazing in polymers, plasticity in metals) and on up to the scale of the structure itself (e.g., large cracks and buckling modes).

Our shortcomings in tackling such a problem are not merely in computational power; the more decisive challenge is to categorize and characterize the many possible mechanisms of damage and build them into a model in a realistic way. Even in a mainly empirical approach to predicting failure, great care must be taken to assure that tests are conducted that will reveal all mechanisms that might appear in service. The history of disasters is replete with cases where the critical mechanism eluded the test regimen. When prediction is taken up as a theoretical challenge, we need not only to know all the mechanisms but also to have a model for each that will correctly represent its effect on the progression to failure.

[1]Teledyne Scientific Co., 1049 Camino Dos Rios, Thousand Oaks, CA 91360, USA. [2]Department of Mechanical and Aerospace Engineering, University of Miami, Coral Gables, FL 33124, USA.

*To whom correspondence should be addressed. E-mail: bcox@teledyne.com

Bottom-Up and Top-Down Models

Current research devolves broadly into two approaches to failure prediction, the bottom-up and the top-down methods. The bottom-up method, which from the first era of fracture and dislocation theory in the mid-20th century has attracted as many physicists as engineers [e.g., (*5*)], seeks to simulate failure by building up detailed models of atomic and molecular processes by means of quantum mechanics and classical molecular dynamics. Processes modeled with increasing realism include crystal plasticity (*6*–*8*), bond rupture in relatively brittle materials for simple crack geometries (*9*–*11*), and the deformation of collagen molecules and fibrils in natural composites (*12*, *13*). The difficulty with the bottom-up method is that the intervals of time and the size of the material that can be modeled remain many orders of magnitude below the duration of a test and the size of a structural test coupon, let alone a structure; therefore, the mechanisms that may be revealed by the model (rather than written into the model explicitly) cannot be guaranteed to be exhaustive of those that arise in large-scale, long-duration experiments. Although bottom-up simulations yield increasingly breathtaking images of small-scale failure mechanisms, they continue to fall well short of representing the complex evolution of damage toward failure in engineering materials.

The top-down method focuses on engineering necessity: Broadly speaking, it seeks always to satisfy the constraint imposed at the structural scale that the displacement fields predicted for given boundary loads match those measured in tests. This can, of course, always be assured for single cases by curve-fitting data; cleverness enters in embellishing the models with representations of the physics of failure that allow prediction for cases (loads and geometry) that have not been tested. The top-down method begins with a macroscopic engineering model, which is progressively augmented by incorporating just those successive levels of detail that are necessary to account for features of engineering tests. Because the model is always calibrated against engineering tests, predictions are available to designers at any stage of model augmentation, subject to some current set of restrictions. Partly for this utility, the top-down method has historically been attractive to engineers. The process of continually validating predictions against tests also rapidly distinguishes those mechanisms or those parameters incorporated in models of mechanisms that have an important effect on engineering performance from those that are irrelevant. This distinction is of practical importance as engineering performance usually depends on only a handful of degrees of freedom, whereas many tens of parameters are commonly proposed in models of mechanisms.

There is much merit in exploring top-down and bottom-up methods concurrently. A profitable strategy is to use the sensitivity analyses of the top-down method to point to those mechanisms for which modeling at finer scales might be pursued, while using the results of bottom-up research to yield the optimal parametric forms to be used when representations of mechanisms are to be incorporated in a top-down model. Regrettably, top-down and bottom-up methods have generally been pursued as distinct exercises by distinct communities, with only occasional serious efforts reported of the transfer of information from one to the other.

In the past decade, research on hierarchical and multiscale models has offered formulations for formally linking top-down and bottom-up approaches in single codes (*13*–*17*). These developments have focused on the mathematical issues of how to embed calculations representing fine-scale phenomena in calculations representing larger-scale phenomena. The mathematical challenges include devising hierarchical meshing strategies that are coarse enough at the largest scales to cover perhaps an entire structure, while cascading down through finer and finer meshes perhaps as far as the atomic scale; integrating classical continuum mechanics calculations with molecular dynamics and even quantum mechanical calculations; and the various boundary-matching problems associated with integrating models executed over different time scales and built on meshes of different gauges.

Hybrid Stress-Strain and Traction-Displacement Models

In continuum (nonatomistic) representations of material damage, two forms of constitutive relation are useful. When spatially continuous

changes arise in the material, including nonlinearity, rate, history, and cycle dependence, the deformation is represented by a constitutive relation between the stress and strain tensors, $\bar{\sigma}\,\bar{\varepsilon}$ (with this abbreviated notation understood to include dependence on time, history, etc.). The law $\bar{\sigma}\,\bar{\varepsilon}$ includes the special case of elasticity and may also include irreversible damage, which appears as hysteresis. The development of relations, $\bar{\sigma}\,\bar{\varepsilon}$, that describe the effects of various kinds of fine-scale damage, including diffuse microcracks, dislocations, and polymer crazing, is the field known as continuum damage mechanics; in this method, discrete damage mechanisms are represented by their effects averaged over suitable gauge lengths, larger than the individual events but small relative to the representative material volume. The second form of constitutive law depicts a discontinuity (or very large gradient) in the material displacement as a localized damage band. A traction-free crack is a familiar special case of a damage band with fully failed material. More generally, the damage band is a mathematically generalized crack across which stresses continue to be transmitted by partially failed material. Although the band in reality may have a finite width, simplification without loss of accuracy (in many cases) can be achieved by representing it as a two-dimensional surface, all the nonlinearity being collapsed into a displacement discontinuity across that surface. As the crack opens, vector tractions, **p**, applied to the crack surfaces equilibrate stresses in the bulk material. The needed constitutive law is the relation **p**(**u**) between **p** and the displacement discontinuity, 2**u**. This relationship is often called a cohesive model.

Materials exhibiting any combination of damage mechanisms can be modeled at the continuum level by hybrid stress-strain and traction-displacement formulations. Furthermore, using a hybrid formulation leads to highly efficient numerical methods. In top-down modeling, the constitutive laws $\bar{\sigma}\,\bar{\varepsilon}$ and **p**(**u**) are treated as functions to be fitted empirically. Eventually, bottom-up models may predict $\bar{\sigma}\,\bar{\varepsilon}$ and **p**(**u**) from first principles; in the near term, bottom-up models provide functional forms for $\bar{\sigma}\,\bar{\varepsilon}$ and **p**(**u**) that guide the empirical fitting process.

Damage Evolution in Structural Composites

As carbon-fiber composites become the first choice for large commercial aircraft structures, the financial motivation for replacing experimental tests by virtual experiments has increased. Both testing labor costs and design cycle times are targets for heavy reduction. But beyond cost, virtual tests also offer the interesting possibility of liberating the design space for composite materials. In the most common strong composite materials, fibers are deployed in unidirectional plies (plies within which all fibers have a common orientation), which are stacked in angled orientations to achieve high stiffness and strength in different directions. Because the stiffness and strength of an individual ply are much higher (by a factor of perhaps 50 to 100) in the fiber direction than in the transverse direction, great performance advantage can be realized by tailoring the ply orientations to suit the anticipated load distribution. In the most general laminate concept, fibers that follow curved paths within plies might be preferred (*18*–*20*), for example, to follow load paths around windows or doors. However, the practicalities of current certification methods force designers to restrict themselves not only to unidirectional plies, but also to just a small number of combinations of ply orientations. The problem is that in an entirely empirical certification system, each variant of ply orientations must be regarded as a distinct material, for which the entire matrix of certification tests must be repeated. If curved fiber paths were used, then in principle an infinite number of different materials would be present in a single structure and certification by empirical methods makes no sense at the material level; certification and the entire range of tests must be done at the level of the entire structure, one candidate fiber pattern at a time!

Thus, structural engineers, limited to ~10^4 tests to certify safety, shy away from complexity, preferring the simplest material solutions that can reasonably do the job (*21*). Simulations that are sufficiently realistic to act as virtual experiments could relax the need for simplicity by vastly increasing the number of tests that can be rapidly and cheaply executed. The essential question, of course, is in how much detail failure mechanisms need to be simulated for a virtual test to give the same engineering outcome as a real test. Minimum requirements are to predict the shape and size of the main crack systems correctly; these dictate the global compliance of the specimen (deflection for given load) and the path to ultimate failure.

The experiments of Figs. 1A and 2A (*22*, *23*) typify laminate material specimen tests in size and ply orientations (0°/90° and 0°/ ±45°/90°). The slot-shaped stress concentrator is often used to represent the kind of severe damage that might be inflicted by a service accident. The circular hole is commonly cut into composite structures to pass bolts, hydraulic and electrical lines, etc. The stress concentrators and potentially the lateral edges of the specimen are sites at or near which damage is likely to initiate. The damage mechanisms shown in Figs. 1A and 2A are some of the most im-

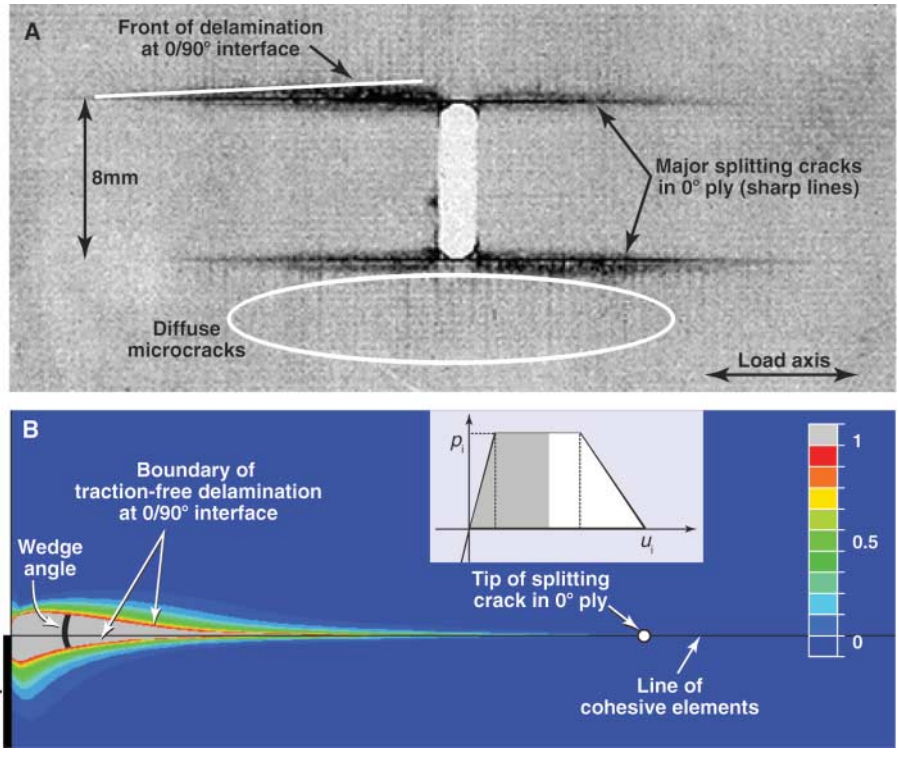

Fig. 1. (**A**) X-ray radiography reveals damage mechanisms viewed through the ply stack in a laminated fibrous polymer composite containing aligned (0°) and transverse (90°) fiber plies loaded in tension (*22*). Dominant splitting cracks appear as sharply defined horizontal lines (in an H configuration) and eventually span the specimen, tending to isolate the strip containing the slit; wedge-shaped delaminations between the plies appear as areas of shadow around the splitting cracks; and myriad microcracks appear between fibers in the transverse plies. (**B**) Plot of level of damage in cohesive model elements between 0° and 90° plies (blue, elastic material; gray, failed material). Inset shows form of cohesive law, for variables defined in text.

portant for tensile loading: splitting cracks, which develop as shear failures; delaminations between plies; and diffuse microcracks running in the fiber direction within individual plies. All of these mechanisms have important effects on the load the composite supports for a given boundary displacement. Splitting and delaminations, together with fiber fractures (which have not yet occurred in Figs. 1A and 2A), also provide paths to ultimate failure. A necessary (minimum) condition for a simulation to be sufficiently realistic is that the evolution of splitting cracks, delaminations, and diffuse microcracking be correctly predicted for arbitrary loads, choices of ply orientation, and shape of the stress concentrator.

Historically, simulations of such notched coupon tests have foundered on some conceptual difficulties with the traditional representations of cracks when they are applied to composites. A very successful model of the elasticity of laminated fibrous composites has been laminate analysis, in which individual plies are homogenized (i.e., the spatial variations in elasticity due to the individual fibers are averaged out) but the heterogeneity from ply to ply is retained. However, in the presence of a free edge, such as at the periphery of a cutout, the ply heterogeneity implies that a singularity must exist in the elastic fields at ply interfaces (*24*). The singular fields (strain energy concentrations) suggest correctly that the interfaces will be the sites of cracking, but the question of how to model the first damage and its progression into a delamination crack of detectable size has proven very thorny.

In linear elastic fracture mechanics (LEFM), which is the traditional model of cracking in nonductile materials, an idealized traction-free crack is assumed and all the material toughness that resists crack advance (the fracture toughness) is assigned to a point process located at the crack tip (Fig. 3); the rest of the body is assumed to be linear-elastic. The beauty of LEFM is that for cracks that are relatively large, the fracture toughness proves to be a material constant, and LEFM, once calibrated, can predict the external loads at which the crack tip conditions will cause crack propagation for any component geometry. LEFM has been remarkably successful in engineering design, including the design of composites, provided a sufficiently large crack is already present. Conservative and therefore safe design can be achieved by assuming that a crack big enough to be detected in service inspections is present and requiring that the load that LEFM predicts for crack propagation exceeds service loads. However, creating realistic damage simulations requires much more than this. The initiation of damage at stress-concentrating sites must be predicted for parts that contain no cracks, and the gradual evolution of initiated damage into large cracks must be modeled.

The critical conceptual limitation of LEFM is representing all the material nonlinearity during crack extension as a point process. In fact, the zone of nonlinearity always has finite size. Nonlinear fracture models, and in particular the cohesive zone idealization, describe the development of the zone of nonlinearity explicitly (Fig. 3) (*25*–*29*).

Modeling Multiple Mechanisms

Various modeling attempts in the recent literature (*30*–*37*) have led to an initial list of necessary model features for simulating notched laminate failure under tensile loads, judged according to the top-down philosophy by whether the attempt has succeeded or failed to reproduce engineering tests. A summary of necessary features can be illustrated through simulations of the tests of Figs. 1A and 2A (*37*). The simulations are based on the finite element method, which computes stress distributions for generic geometry and loads. Special model features are embedded within the finite element formulation by the use of custom elements and nonlinear constitutive laws.

In these simulations, delamination damage is modeled by a cohesive model with a reasonable functional form for $\mathbf{p}(\mathbf{u})$ [Fig. 1B, inset; $u_1 \geq 0$; $p_i(u_i) = -p_i(-u_i)$, $i = 2, 3$, where p_i and u_i are components of $\mathbf{p}$ and $\mathbf{u}$ and the Cartesian coordinates 2 and 3 lie in the plane of the crack] independently determined by the analysis of polymer adhesives in de-adhesion experiments (*38*). The cohesive model is incorporated in the simulations by special interface elements, which allow a displacement discontinuity when the local stress satisfies a critical condition. The elements are planted over all ply interfaces to allow the possibility of ply delamination with nonprescribed delamination shape. In the first simulations to be described, they are also planted along the planes within the 0° plies that are tangent to the ends of the slot, where the dominant splitting cracks occur in Fig. 1A. A key feature of the cohesive model is that it allows arbitrary mixed-mode crack tip conditions—that is, arbitrary proportions of opening and sliding displacements across the nonlinear process zone—which can (and do) vary along a crack front. Calculating the separation of the energy released by crack advance into contributions attributable to crack opening and sliding, which is prerequisite to predicting the condition for crack

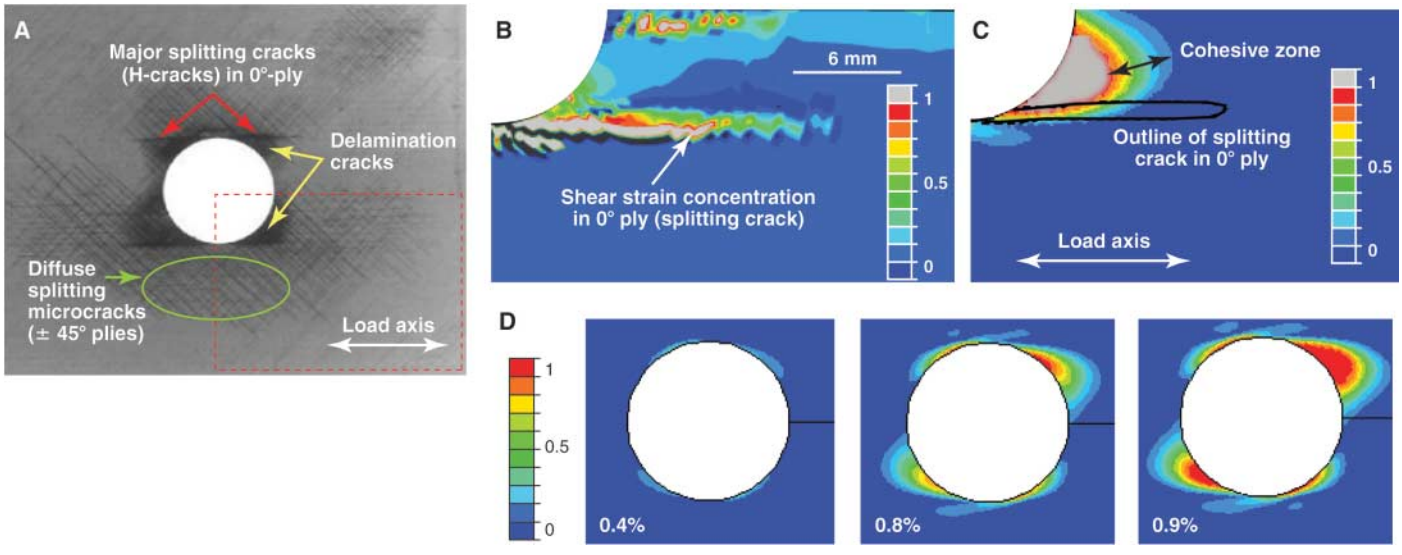

Fig. 2. (**A**) Images similar to Fig. 1 for a laminate that also contains angled (±45°) fiber plies and a circular hole instead of a slit (*23*). The splitting cracks are now shorter, the delaminations are no longer wedge-shaped but lobe-shaped, and diffuse microcracking occurs predominantly in the ±45° plies. (**B**) Computed continuum damage distribution in 0° ply (blue undamaged; gray is completely failed material) showing shear strain concentration that forms splitting crack. (**C**) Computed damage in cohesive zone between 0° and 45° plies (blue is undamaged; gray is completely failed material). (**D**) Initiation and evolution of damage in cohesive zone between 0° and 45° plies at marked applied strains. Blue is undamaged material; red is completely failed (traction-free).

propagation, is very troublesome for cracks of general shape in the LEFM formulation, implemented for example via the virtual crack closure technique. In a cohesive model formulation, the energy partition is immediately deducible from the opening and sliding displacements, which are computed automatically as part of the finite element problem. A suitable failure criterion built into the cohesive model then allows automatic calculation of the evolution of crack shape (*37*).

Diffuse microcracking, which may occur in any ply, is modeled by assigning a nonlinear constitutive law, $\bar{\sigma}\,\bar{\varepsilon}$, to the ply material that causes material degradation (softening) according to a continuum damage model. Many models of reasonable functional form are available to represent this effect [e.g., (*39*, *40*)].

Even though the specimens of Figs. 1 and 2 are thin sheets loaded in-plane, opening displacements arise when cracking occurs. Therefore, accurate calculation of the crack displacements requires that the full three-dimensional stress state be calculated. Plate elements, which have been very popular in laminate analysis because they greatly reduce the number of degrees of freedom in a calculation, are not adequate; three-dimensional finite elements should be used. For mesh-independent results, these elements must not be larger than the nonlinear process (cohesive) zones that arise at crack tips during a calculation, which in a typical aerospace carbon-epoxy laminate are ~0.3 to 1 mm. Fortunately, the zone lengths can be estimated in advance from analytical cohesive model results (*27*, *37*, *41*), avoiding the need for iterative mesh refinement. If integrations are performed with carefully developed numerical methods, especially where cohesive zones extend partway across an element, then it is sufficient for the three-dimensional elements used for plies to be commensurate with (rather than smaller than) the cohesive zone lengths (*37*).

Simulations that follow all these rules (a qualification that excludes most of the literature) are encouragingly successful. The wedge-like shape of the delamination cracks in the 0°/90° laminate is reproduced, with comparable wedge angle (allowing uncertainty about how far the dye penetrant used in the x-ray measurements infiltrated the damage zone), and the length of the splitting cracks is in approximately the correct proportion to the delamination size. Other plots show that the distribution of diffuse microcracking in the 90° plies is predicted correctly within the uncertainty of the image resolution.

The importance of mutual interactions among different failure mechanisms due to the effect of each on the stress field experienced by the others can quickly be shown by turning off one mechanism in a simulation (*36*, *37*). Thus, for example, when ply nonlinearity is omitted from the calculation, the delaminations of Fig. 1A are predicted incorrectly to grow mainly between the dominant splitting cracks instead of outside them (*37*). When ply nonlinearity is included, the zone in the 90° ply in which it is concentrated coincides with the area of the delamination between the 0° and 90° plies at any instant.

The instructive possibility of nonuniqueness in formulating a model that is sufficient from the top-down view is highlighted in the simulations of the test of Fig. 2A. In these simulations, no cohesive elements were planted along the crack paths that are expected to be followed by splitting cracks. But a manifestation of the splitting cracks still arises: A shear damage band has formed in the same locations (Fig. 2B), mediated by the continuum deformation introduced by the relation $\bar{\sigma}\,\bar{\varepsilon}$ assigned to the 0° plies. Provided $\bar{\sigma}\,\bar{\varepsilon}$ includes the possibility of material failure, the damage band is not only highly localized (because of instability in the local stress state caused by the stress-concentrating hole) but also can evolve into a traction-free crack. From the point of view of the fine-scale material behavior, a discrete crack model and a continuum damage representation are very different. But the outcome at the level of the engineering performance of the structure in this particular case is much the same.

The level of fidelity shown in Figs. 1 and 2 is a recent accomplishment (*37*). When the ply orientations and hole shape are changed, the same model used in Fig. 1, without any parameter modification other than the choice of representing splitting cracks, correctly predicts the new damage patterns (Fig. 2, B and C), especially the lobe shape of the delaminations and their size in proportion to that of the splitting cracks. In contrast, prior model formulations failed to reproduce crack shapes correctly, usually because the mesh choice did not satisfy the requirement of not being larger than the damage zones, so that the ratio of sliding to opening displacement across the zone could not be predicted, or the three-dimensional stress state was not fully modeled, or the interactions between all three mechanisms present in the experiments were not considered.

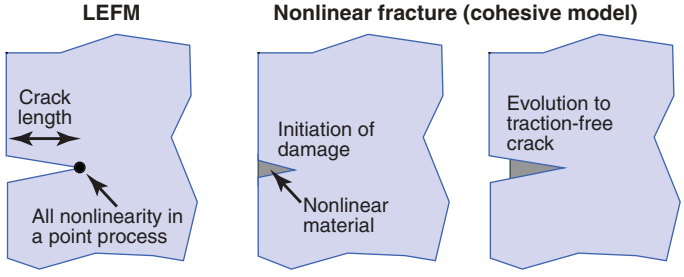

Fig. 3. According to linear elastic fracture mechanics (LEFM), the applied load required to evolve damage (grow the crack) tends to infinity as the crack length approaches zero. In a cohesive model, the applied load for damage initiation and evolution is limited to some finite multiple of the maximum value p_{max} of a component of the assigned cohesive law **p**(**u**).

The cohesive model of delamination provides a unifying physical model of damage initiation and its progression to large cracks (Fig. 2D) and is an important conceptual advance in damage modeling. Initiation sites are determined by local stress conditions; the delamination damage zones then extend both around and away from the stress concentrator, until the displacement discontinuity vector exceeds the critical condition for forming a traction-free zone. When the traction-free zone becomes large enough, the limit in which LEFM is valid is approached and the two models become equivalent.

The simulations of Figs. 2 and 3 are only part of the whole story: Given the state of damage predicted for the initial tensile load, one can then restate the boundary conditions to ask how damage will evolve for other subsequently applied load types, including compression and twist. The application of compression after loads that have caused delamination is particularly dangerous: Local ply buckling causes further delamination growth and is a primary failure mode for damaged airframes and marine structures. The critical compressive load for ply buckling is approximately inversely proportional to the delamination size and depends on the delamination shape.

The Extended Finite Element Method: Dynamic Crack Path Selection

For splitting cracks originating at notch extremities and delamination cracks, the potential crack paths are known a priori because they are constrained by the geometry of either the material or the specimen. Other crack systems, including splitting cracks in specimens of more complicated geometry, shear bands, and distributed intraply matrix cracks, follow paths that are determined during damage evolution by changes in the local stress fields. An important advance in finite element formulations, the extended finite element method (XFEM), defines solid continuum elements within which a general displacement discontinuity can be introduced if some failure criterion is satisfied in the element at any time during a simulation (*42*–*44*). The displacement discontinuity can appear on any plane in the element and can be associated with tractions, **p**. Thus, cracks described by a cohesive crack model can appear in any number and follow any path during a simulation, determined by the evolving stress distribution. Crack branching and mother-daughter crack systems can appear. Implementation of three-dimensional elements in the XFEM formulation is a current research activity and will soon add an important empowerment to damage simulations.

Calibration and Validation

Even as the successful prediction of delamination crack shapes shown in Figs. 1 and 2 encourages the quest for virtual experiments, designers require

simple methods of calibrating and validating the nonlinear constitutive laws, $\mathbf{p}(\mathbf{u})$ and $\bar{\sigma}\bar{\varepsilon}$. The cohesive law is especially challenging, because it refers for polymer composites to nonlinear zones that are ~1 mm or less in size. The inference of $\mathbf{p}(\mathbf{u})$ from the nonlinearity in load-deflection data, which works well for materials with larger cohesive zones of ~10 mm (*45*, *46*), is problematic for a 1-mm zone because specimen deflections are small during the zone's development. Once the crack is relatively large (well-developed damage zone), its behavior contains no information about $\mathbf{p}(\mathbf{u})$ other than $\int p_i du_i$ (the work of fracture) (*27*, *47*). Alternative experiments that infer $\mathbf{p}(\mathbf{u})$ from crack profiles in plane specimens such as the short shear beam or cantilever beam (*46*, *48*) would need to resolve displacements around cracks that are barely discernible. Thus, none of the common methods in the literature appear immediately workable. New experimental methods for measuring very small crack displacements (e.g., with high-resolution x-ray tomography) are very promising; however, the interpretation of such experiments may prove challenging, which raises the question of whether x-ray tomography can serve as a standard calibration method executed by a field engineer. A simpler prospect may be to use the evolution of the macroscopic crack shape as the calibrating information, because Figs. 1 and 2 suggest that this is an information-rich experiment for determining $\mathbf{p}(\mathbf{u})$. Current research continues to seek a calibration method, validated by testing the accuracy to which ensuing predictions match fracture experiments.

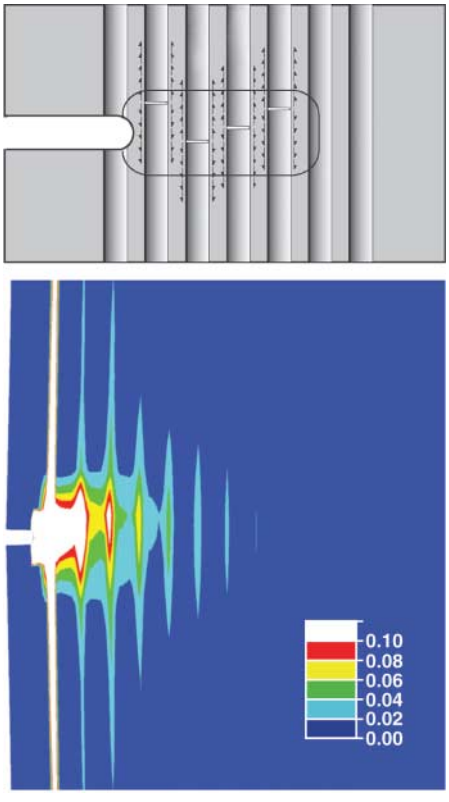

Fig. 4. Simulation of a metal matrix composite failing in bending: stochastic fiber breaks and interfacial sliding (**top**) and accumulated plastic strain (second strain invariant—scale given in key) in the matrix (**bottom**) (*49*).

Fiber Bundle Failure

The tests of Figs. 1 and 2 will ultimately terminate in fiber bundle failure. Simulating fiber failure requires further model augmentation, with a locally refined mesh in which fibers are represented discretely. Constitutive laws must be added at the fiber scale to represent fiber failure, debonding of fibers from the matrix and frictional sliding between the two, and matrix deformation and failure. Thus, a hybrid stress-strain and traction-displacement formulation is again appropriate. In the recent example reproduced in Fig. 4 (*49*) for a metal matrix composite of relatively large SiC fibers in a Ti-6Al-4V alloy matrix, one cohesive model was used to control fiber failure and a second to model fiber-matrix interfacial friction, while continuum laws modeled matrix deformation. (The friction law includes resistance to material interpenetration in the relation between $\mathbf{p}$ and $\mathbf{u}$; sliding resistance is described by a relation between the normal and shear components of $\mathbf{p}$.) The simulation reveals details of the sequence of fiber failure events and the severe matrix deformation that is caused by consequent load shedding. Using material properties known a priori, load-displacement data for a notched bend test could be reproduced, including nonlinearity, ultimate strength, and snap-back phenomena associated with the rupture of individual fibers.

Current Challenges

The ability to link separate resin and fiber properties to the engineering metrics of fiber bundle rupture raises the attractive prospect of predicting the effect of material choice via a virtual experiment. However, this is more complicated than the idealization of Fig. 4 suggests. First, the reality of fibrous reinforcement is that fibers appear in random rather than spatially ordered patterns, with substantial variations in the nearest-neighbor spacing that are not easily quantified. Although this may have a minor effect on fiber rupture under aligned loads, it can dominate the cracking sequence and the statistics of crack initiation under transverse loads (*50*). Second, finer fibers than the SiC fibers of Fig. 4, such as 7-μm carbon fibers, follow paths that are slightly wavy rather than ideally straight. The statistics of fibers that are misaligned over a critical volume exceeding ~1 mm (*51*) control compressive failure via the mechanism of fiber kinking (fiber buckling instability due to fiber rotation) (*52*–*54*). Third, fine fibers tend to mingle from one nominally unidirectional ply to another, forming mechanical bridges across delamination planes, with important consequences for the cohesive tractions that control the delamination. The state of the art of top-down models is that all such stochastic details of microstructure are subsumed in the constitutive laws used in coarser-scale models. To incorporate fiber-level mechanisms in fiber-scale models, substantial research is still required to relate distributions in geometrical and material parameters to the statistics of test data.

One can also contemplate interfacial debonding and the complexity of static and dynamic friction, as well as the molecular-level mechanisms (such as polymer microcracking and crazing) that are the fundamental mechanisms of mixed mode delamination. With the formalism of multiscale methods available, these are the next challenges for creators of virtual experiments. But observe the propensity of top-downers to fit engineering data with a large number of parameters and claim that the resulting model is unique and imbued with predictive power, and that of bottom-uppers to project that their favorite mechanism is the one that propagates up among all others to control engineering behavior. The challenges will not be easily met; beware premature claims of victory.

References and Notes

1. G. Galilei, *Dialogues Concerning Two New Sciences* (Elsevier, Amsterdam, 1636).
2. K. Weighardt, *Z. Math. Phys.* **55**, 60 (1907).
3. A. A. Griffith, *Philos. Trans. R. Soc. London Ser. A* **221**, 163 (1921).
4. A. Fawcett, J. Trostle, S. Ward, paper presented at the 11th International Conference on Composite Materials, Gold Coast, Australia, 1997.
5. P. B. Hirsch, Ed., *Defects* (Cambridge Univ. Press, Cambridge, 1975), vol. 2.
6. F. Abraham *et al.*, *Proc. Natl. Acad. Sci. U.S.A.* **99**, 5777 (2002).
7. M. J. Buehler, H. Gao, in *Handbook of Theoretical and Computational Nanotechnology*, M. Rieth, W. Schommers, Eds. (American Scientific, Stevenson Ranch, CA, 2005), vol. 2, pp. 427–468.
8. W. Cai, V. V. Bulatov, J. Chang, J. Li, S. Yip, in *Dislocations in Solids*, F. N. R. Nabarro, J. P. Hirth, Eds. (Elsevier, Amsterdam, 2004), vol. 12, pp. 1–80.
9. P. Gumbsch, in *Materials Science for the 21st Century* (Society of Materials Science, Kyoto, Japan, 2001), vol. A, pp. 50–58.
10. M. Marder, *Comput. Sci. Eng.* **1**, 48 (1999).
11. F. F. Abraham, *Adv. Phys.* **52**, 727 (2003).
12. J. B. Thompson *et al.*, *Nature* **414**, 773 (2001).
13. M. J. Buehler, *Proc. Natl. Acad. Sci. U.S.A.* **103**, 12285 (2006).
14. W. E. B. Engquist, X. Li, W. Ren, E. Vanden-Eijnden, *Commun. Comput. Phys.*, in press.
15. H. S. Park, *J. Comput. Phys.* **207**, 588 (2005).
16. G. J. Wagner, W. K. Liu, *J. Comput. Phys.* **190**, 249 (2003).
17. M. J. Buehler, *J. Comput. Theor. Nanosci.* **3**, 603 (2006).
18. A. S. Brown, *Aerospace America* (August 1998), pp. 26–28.
19. D. C. Jegley, B. F. Tatting, Z. Gürdal, paper presented at the 44th AIAA/ASME/ASCE/AHS/ASC Structures, Structural Dynamics and Materials (SDM) Conference, Norfolk, Virginia, April 2003.
20. M. W. Tosh, D. Kelly, *Composite Struct.* **53**, 133 (2001).
21. Nature, by contrast, often prefers complexity to achieve safe structures. Consider, for example, the wonderfully complex patterns of twisting, meandering, ganging, and layering seen in the mineralized rods that make up dental enamel, or the richly hierarchical arrangements of collagen and hydroxyapatite found in cortical and trabecular bone. To construct an apology for engineers, we might regard each generation in evolution as a mechanical test, allow vertebrates to have been around for 10^8 years, assume annual reproduction for most of that time, and, conservatively, 10^6 specimens in each

generation, to see that nature has had the benefit of 10^{14} reliability tests to optimize design, conducted without too much regard for the safety of the individual.
22. S. M. Spearing, P. W. R. Beaumont, *Composites Sci. Technol.* **44**, 159 (1992).
23. S. W. Case, K. L. Reifsnider, "MRLife12 Theory Manual—A strength and life prediction code for laminated composite materials" (Materials Response Group, Virginia Polytechnic Institute and State University, 1999).
24. D. B. Bogy, *J. Appl. Mech.* **42**, 93 (1975).
25. G. I. Barenblatt, in *Advances in Applied Mechanics*, H. L. Dryden, T. Von Kármán, Eds. (Academic Press, New York, 1962), vol. 2, pp. 55–129.
26. J. R. Rice, in *Proceedings of The Enrico Fermi International School of Physics*, A. M. Dziewonski, E. Boschi, Eds. (North-Holland, Amsterdam, 1980), vol. 78, pp. 555–649.
27. B. N. Cox, D. B. Marshall, *Acta Metall. Mater.* **42**, 341 (1994).
28. D. S. Dugdale, *J. Mech. Phys. Solids* **8**, 100 (1960).
29. A. Needleman, *Int. J. Fract.* **42**, 21 (1990).
30. R. Borg, L. Nilsson, K. Simonsson, *Composites Sci. Technol.* **64**, 269 (2004).
31. Z. Petrossian, M. R. Wisnom, *Composites A* **29**, 503 (1998).
32. S. T. Pinho, L. Iannucci, P. Robinson, *Composites A* **37**, 63 (2006).
33. J. J. C. Remmers, R. de Borst, A. Needleman, *Comput. Mech.* **31**, 69 (2003).
34. J. C. J. Schellekens, R. de Borst, *Key Eng. Mater.* **121–122**, 131 (1996).
35. G. N. Wells, R. de Borst, L. J. Sluys, *Int. J. Numer. Methods Eng.* **54**, 1333 (2002).
36. M. R. Wisnom, F.-K. Chang, *Composites Sci. Technol.* **60**, 2849 (2000).
37. Q. D. Yang, B. N. Cox, *Int. J. Fract.* **133**, 107 (2005).
38. M. D. Thouless, Q. D. Yang, in *The Mechanics of Adhesion*, D. A. Dillard, A. V. Pocious, M. Chaudhury, Eds. (Elsevier Science, Amsterdam, 2001), vol. 1, pp. 235–271.
39. L. N. McCartney, *Composites Sci. Technol.* **58**, 1069 (1998).
40. K. Y. Chang, S. Liu, F. K. Chang, *J. Composite Mater.* **25**, 274 (1991).
41. R. Massabò, B. N. Cox, *J. Mech. Phys. Solids* **47**, 1265 (1999).
42. N. Moës, J. Dolbow, T. Belytschko, *Int. J. Numer. Methods Eng.* **46**, 131 (1999).
43. T. Strouboulis, K. Copps, I. Babuška, *Comput. Mech. Adv.* **190**, 4801 (2001).
44. N. Moës, T. Belytschko, *Eng. Fract. Mech.* **69**, 813 (2002).
45. U. Stigh, *Int. J. Fract.* **37**, R13 (1988).
46. R. Massabò, D. R. Mumm, B. N. Cox, *Int. J. Fract.* **92**, 1 (1998).
47. L. R. F. Rose, *J. Mech. Phys. Solids* **35**, 383 (1987).
48. B. N. Cox, D. B. Marshall, *Int. J. Fract.* **49**, 159 (1991).
49. C. González, J. Llorca, *Acta Mater.* **54**, 4171 (2006).
50. D. B. Marshall *et al.*, *Acta Metall. Mater.* **42**, 2657 (1994).
51. N. A. Fleck, J. Y. Shu, *J. Mech. Phys. Solids* **43**, 1887 (1995).
52. A. S. Argon, *Fracture of Composites*, Treatise of Materials Sciences and Technology (Academic Press, New York, 1972), vol. 1.
53. B. Budiansky, *Composite Struct.* **16**, 3 (1983).
54. N. A. Fleck, B. Budiansky, in *Inelastic Deformation of Composite Materials*, G. J. Dvorak, Ed. (Springer-Verlag, New York, 1991), pp. 235–274.
55. Supported by Army Research Office Agreement W911NF-05-C-0073. We thank T. Belystchko, M. Buehler, J. Llorca, R. Massabò, M. Spearing, J. Whitcomb, and two anonymous reviewers for critical comments.

10.1126/science.1131624

REVIEW

Nanoparticle Polymer Composites: Where Two Small Worlds Meet

Anna C. Balazs,[1] Todd Emrick,[2] Thomas P. Russell[2]*

The mixing of polymers and nanoparticles is opening pathways for engineering flexible composites that exhibit advantageous electrical, optical, or mechanical properties. Recent advances reveal routes to exploit both enthalpic and entropic interactions so as to direct the spatial distribution of nanoparticles and thereby control the macroscopic performance of the material. For example, by tailoring the particle coating and size, researchers have created self-healing materials for improved sustainability and self-corralling rods for photovoltaic applications. A challenge for future studies is to create hierarchically structured composites in which each sublayer contributes a distinct function to yield a mechanically integrated, multifunctional material.

The mixing of nanoparticles with polymers to form composite materials has been practiced for decades. For example, the clay-reinforced resin known as Bakelite was introduced in the early 1900's as one of the first mass-produced polymer-nanoparticle composites (*1*) and fundamentally transformed the nature of practical household materials. Even before Bakelite, nanocomposites were finding applications in the form of nanoparticle-toughened automobile tires prepared by blending carbon black, zinc oxide, and/or magnesium sulfate particles with vulcanized rubber (*2*). Despite these early successes, the broad scientific community was not galvanized by nanocomposites until the early 1990s, when reports by Toyota researchers revealed that adding mica to nylon produced a five-fold increase in the yield and tensile strength of the material (*3*, *4*). Subsequent developments have further contributed to the surging interest in polymer-nanoparticle composites. In particular, the growing availability of nanoparticles of precise size and shape, such as fullerenes, carbon nanotubes, inorganic nanoparticles, dendrimers, and bionanoparticles, and the development of instrumentation to probe small length scales, such as scanning force, laser scanning fluorescence, and electron microscopes, have spurred research aimed at probing the influence of particle size and shape on the properties of nanoparticle-polymer composites.

As part of this renewed interest in nanocomposites, researchers also began seeking design rules that would allow them to engineer materials that combine the desirable properties of nanoparticles and polymers. The ensuing research revealed a number of key challenges in producing nanocomposites that exhibit a desired behavior. The greatest stumbling block to the large-scale production and commercialization of nanocomposites is the dearth of cost-effective methods for controlling the dispersion of the nanoparticles in polymeric hosts. The nanoscale particles typically aggregate, which negates any benefits associated with the nanoscopic dimension. There is a critical need for establishing processing techniques that are effective on the nanoscale yet are applicable to macroscopic processing. Another hurdle to the broader use of nanocomposites is the absence of structure-property relationships. Because increased research activity in this area has only spanned the past decade, there are limited property databases for these materials (*5*). Thus, greater efforts are needed to correlate the morphology of the mixtures with the macroscopic performance of the materials. Establishing these relationships requires a better understanding of how cooperative interactions between flexible chains and nanoscopic solids can lead to unexpected behavior, like the improved mechanical behavior of mica-reinforced nylon.

The interactions of nanoparticles with polymers are mediated by the ligands attached to the nanoparticles; thus, the ligands markedly influence particle behavior and spatial distribution. Therefore, we first describe recent advances in nanoparticle surface modification and then the interactions between these particles and polymer matrices, including homopolymers, diblock copolymers, and blends.

Surface Functionalization of Nanoparticles

The surface chemistry of nanoparticle functionalization evolved in part from studies on functionalized planar surfaces, including self-assembled monolayers (SAMs) (*6*) and polymer brushes (*7*) on substrates ranging from gold to metal oxides. As with planar substrates, functional small molecules and polymers can be attached to nanoparticles by physical adsorption or covalent attachment. Synthetic strategies that give polymer-functionalized nanoparticles include performing the particle synthesis directly in the polymer matrix, replacing small-molecule ligands inherent to a nanoparticle synthesis with functional polymers in a "grafting-to" process, and growth of polymers from functionalized nanoparticles in a "grafting-from" process. It is imperative, though, that the conditions used retain the specific characteristics of the nanoparticles.

Many state-of-the-art nanoparticle preparations afford high-quality particles by decomposition of organometallic precursors in a solution environment that leads to surface coverage with small-molecule alkane-based ligands, like *n*-alkyl thiols, amines, or

[1]Department of Chemical and Petroleum Engineering, University of Pittsburgh, Pittsburgh, PA 15261, USA. [2]Polymer Science and Engineering Department, University of Massachusetts, Amherst, MA 01003, USA.

*To whom correspondence should be addressed. E-mail: russell@mail.pse.umass.edu